doi:10.1017/S1431927621009028
Microsc. Microanal. 27 (Suppl 1), 2021

High porosity fine-grained rims in CM Murchison revealed through sub-resolution XCT imaging with Xe gas

Romy Hanna, Rich Ketcham and Dave Edey

University of Texas at Austin, Austin, Texas, United States

Fine-grained rims (FGRs) are dust-sized material that surrounds chondrules and refractory inclusions in chondritic meteorites. Multiple lines of theoretical, experimental, and empirical evidence point to their formation from the accretion of nebular dust onto chondrule surfaces prior to the formation of chondrite parent bodies [e.g., 1-4]. Recently, we have applied X-ray computed tomography (XCT) to examine the 3D morphology of FGRs, finding that the chondrule size to rim volume relationship is consistent with their formation in a turbulent, rather than laminar, nebular setting [3]. Modeling studies have suggested that the internal porosity structure of the FGRs is also dependent on nebular conditions such as the degree of turbulence and grain charge [5, 6]. However, the size of pores within FGRs is submicron- to micron-sized, and studies so far have utilized scanning electron microscopy (SEM) which limits the volume of observation and provides only a 2D picture of the porosity structure. As a 3D imaging technique, XCT is well suited to get around the 2D observational limitation, but the small size of the pores still necessitates a small volume (< ~1 mm^3) using traditional XCT imaging.

A specialized XCT technique pioneered in the oil and gas industry, however, provides a more complete characterization of material structure and porosity at a scale below the imaging resolution [7]. By XCT imaging a porous sample twice, once dry and once infiltrated by a gas or fluid, and then subtracting the former from the latter, one obtains a 3D map of where the fluid or gas infiltrated, and thus the porosity. In such maps, each voxel value corresponds to partial porosity, or the fraction of the voxel that contains pore space, thus revealing the location of all interconnected porosity, at all scales. This approach retains the ability to measure large, discrete pores, while simultaneously revealing all smaller-scale porosity and its lithologic and textural associations and structure, for samples of any size. The approach was initially developed for fluid infiltration imaged with medical CT [7] and subsequently adapted to microCT [e.g., 8] to provide detailed maps of porosity structure in complex lithologies. We have recently begun to apply this technique to examine the distribution of porosity within carbonaceous chondrites using the heavy noble gas Xenon which is highly attenuating to X-rays. Its chemical nonreactivity also allows inspection of extremely fine-scale porosity in chondrites that would otherwise alter or swell in the presence of a fluid.

For our first measurement we mounted a 0.143 g chip (~4 mm widest diameter) of CM Murchison (Chip A of [3]) within an aluminum pressure vessel and imaged it on our Zeiss Xradia microXCT scanner on the 4x detector at 90 kV, 10W using 1801 projections for a total scan time of 7.1 hours. We then pumped the sample chamber to a low vacuum, flooded the vessel with Xe gas at 24 atm, and repeated the scan with the same acquisition parameters. The final reconstructed voxel size for both scans was 5.00 µm. Because Xe completely surrounded the chip it filtered the X-ray beam (which is polychromatic – i.e., composed of many X-ray energies, with a maximum energy of 90 keV but a mean closer to 50 keV) and modified the X-ray attenuation response of the non-porous materials (olivine, sulfides) within the sample. We therefore re-scaled the Xe-filled data volume so the attenuation (CT numbers) of these non-porous materials matched that of the air-filled scan, rigidly aligned the two scan volumes in Avizo™, and then subtracted the images to get the data volume of the relative Xe gas abundance (Fig. 1). As expected, the Xe abundance is highest in the space surrounding the sample (Fig. 1c; the visible lines are that of a Kimwipe™ that wrapped the sample to secure it within the tube) and the lowest Xe abundance is within the chondrules, although noise is a significant issue. However, we can still discern variation in microporosity within the sample, most interestingly that a large portion of the FGRs which surround the chondrules have a higher microporosity than the matrix (Fig. 1). This is consistent with a previous study that examined microporosity (via PFIB-SEM sectioning) in CM EET 96029 and found a higher porosity for the FGR than the nearby matrix [9], although the porosity difference between rims and matrix in CM Murchison appears to be much higher. More importantly, however, we are able to examine the porosity distribution in 3D and within larger volumes than allowed via an SEM approach.

To reduce noise, we have built a sample chamber of PEEK (polyether ether ketone; an engineered polymer) which has a significantly lower X-ray attenuation than aluminum. A rescan of the chip in this tube with the same parameters (but without Xe gas) resulted in a substantial decrease in noise (Fig. 2A,B). The scan was also significantly faster as it was acquired on our new scanner (Zeiss Versa 620 installed in January 2020), with a total scan time of 1.85 hours. We also demonstrate the ability of the Versa 620 to image subvolumes at higher resolution (Fig. 2C), providing further textural context to porosity measurements, such as association with microfractures. We are currently completing construction of the PEEK rig to scan the chip with pressured Xe to obtain a new dataset with reduced noise to more accurately characterize the porosity and structure of the FGRs.

Funding Acknowledgement

This work is funded through the NASA Laboratory Analysis of Returned Samples program.

https://doi.org/10.1017/S1431927621009028 Published online by Cambridge University Press

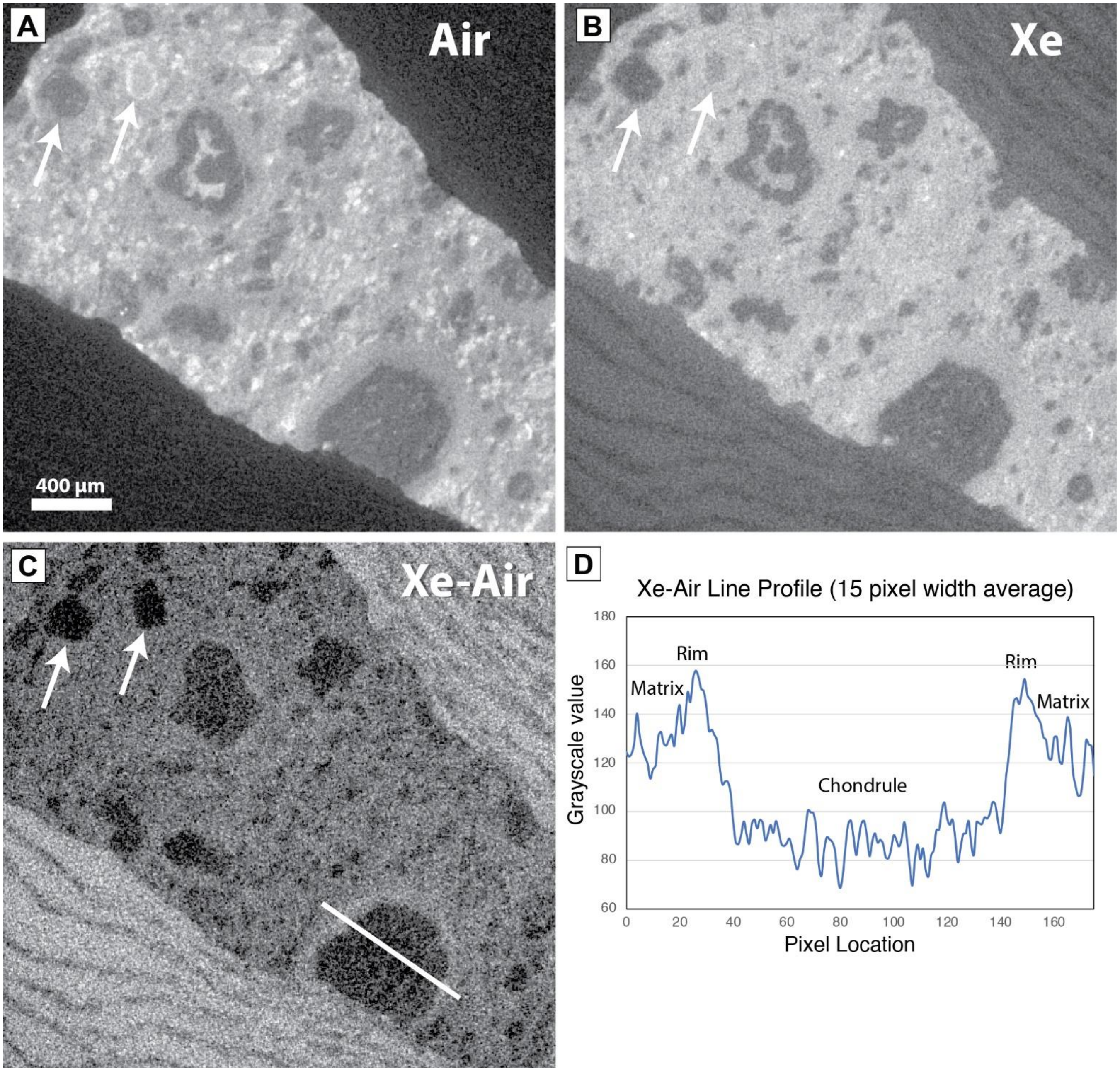

Figure 1. Figure 1: XCT scans of Murchison chip; all 5 µm/voxel (same scale for XCT images A-C). (A) Scan in air (B) Scan in Xe (C) Aligned and subtracted image (Xe-Air). White arrows indicate two chondrules with differing compositions (see A) that are both non-porous. White line is line profile in D. (D) The chondrule's fine-grained rim is more porous than the surrounding matrix, which also has significantly more porosity compared to the chondrule. This increased porosity is easily visible in the subtraction image (C) although the individual pores are well below the resolution of the scan (A and Fig. 2).

https://doi.org/10.1017/S1431927621009028 Published online by Cambridge University Press

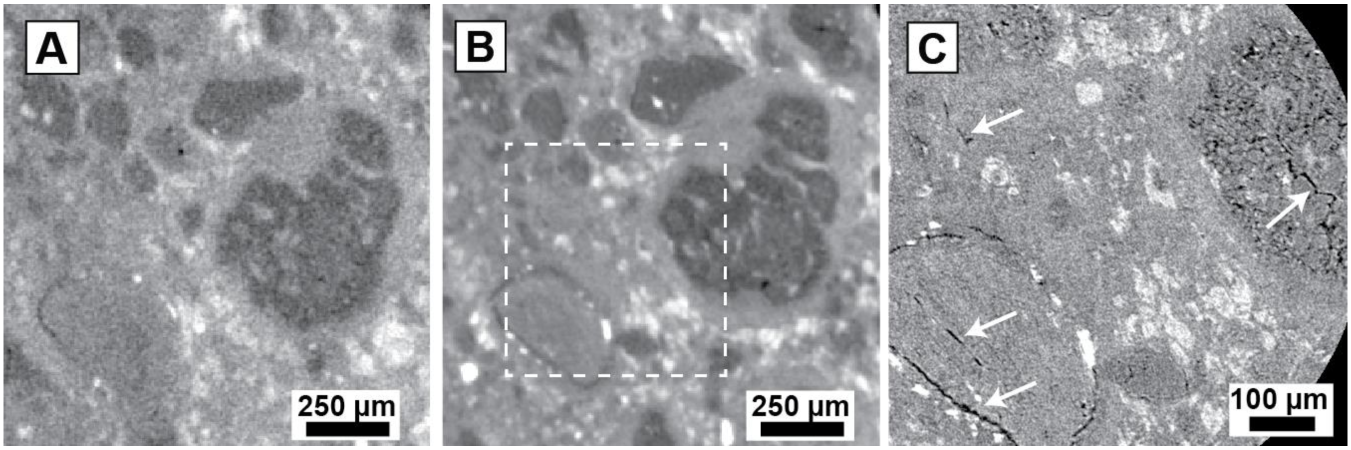

Figure 2. Figure 2: XCT scans of Murchison chip. (A) 5 µm/voxel scan on 4x detector in Al tube (same data as shown in Fig. 2A). (B) 5 µm/voxel scan on 4x detector in PEEK tube. There is a substantial decrease in noise due to the lower X-ray attenuation of PEEK compared to Al. (C) 1 µm/voxel subvolume scan on the 20x detector in PEEK tube. Several micron-sized pores are now apparent (white arrows), although it is confirmed that the majority of porosity within the FGRs are well below 1 micron in size.

References

1. Cuzzi, J.N., *Blowing in the wind: III. Accretion of dust rims by chondrule-sized particles in a turbulent protoplanetary nebula.*Icarus, 2004. **168**(2): p. 484-497.
2. Metzler, K., A. Bischoff, and D. Stoeffler, *Accretionary dust mantles in CM chondrites - Evidence for solar nebula processes.*Geochimica et Cosmochimica Acta, 1992. **56**: p. 2873-2897.
3. Hanna, R.D. and R.A. Ketcham, *Evidence for accretion of fine-grained rims in a turbulent nebula for CM Murchison.*Earth and Planetary Science Letters, 2018. **481**: p. 201-211.
4. Beitz, E., et al., *Experimental investigation of the nebular formation of chondrule rims and the formation of chondrite parent bodies.*Geochimica et Cosmochimica Acta, 2013. **116**: p. 41-51.
5. Xiang, C., et al., *The initial structure of chondrule dust rims I: Electrically neutral grains.*Icarus, 2019. **321**: p. 99-111.
6. Xiang, C., et al., *The initial structure of chondrule dust rims II: Charged grains.*Icarus, 2021. **354**: p. 114053.
7. Wellington, S.L. and H.J. Vinegar, *X-Ray Computerized Tomography.*Journal of Petroleum Technology, 1987. **39**(08): p. 885-898.
8. Ketcham, R.A. and G.J. Iturrino, *Nondestructive high-resolution visualization and measurement of anisotropic effective porosity in complex lithologies using high-resolution X-ray computed tomography.*Journal of Hydrology, 2005. **302**(1): p. 92-106.
9. Daly, L., et al. *Porosity Variations Between Fine Grained Rims and Matrix in a CM Chondrite by 3D Serial Sectioning*. in *Lunar and Planetary Science Conference XLIX*. 2018. Houston, TX.